HAL
open science

Expansion of an ultra-cold lithium gas in the BEC-BCS crossover

Leticia Tarruell, Martin Teichmann, Jason Mckeever, Thomas Bourdel, Julien Cubizolles, Lev Khaykovich, Jing Zhang, Nir Navon, Frédéric Chevy, Christophe Salomon

To cite this version:

Leticia Tarruell, Martin Teichmann, Jason Mckeever, Thomas Bourdel, Julien Cubizolles, et al.. Expansion of an ultra-cold lithium gas in the BEC-BCS crossover. 2007. hal-00123470

HAL Id: hal-00123470

https://hal.science/hal-00123470

Preprint submitted on 9 Jan 2007

HAL is a multi-disciplinary open access archive for the deposit and dissemination of scientific research documents, whether they are published or not. The documents may come from teaching and research institutions in France or abroad, or from public or private research centers.

L'archive ouverte pluridisciplinaire **HAL**, est destinée au dépôt et à la diffusion de documents scientifiques de niveau recherche, publiés ou non, émanant des établissements d'enseignement et de recherche français ou étrangers, des laboratoires publics ou privés.

hal-00123470, version 1 - 9 Jan 2007

Expansion of a lithium gas in the BEC-BCS crossover

L. Tarruell[1], M. Teichmann[1], J. McKeever[1], T. Bourdel[1], J. Cubizolles[1], L. Khaykovich[2], J. Zhang[3], N. Navon[1], F. Chevy[1], and C. Salomon[1]

[1] *Laboratoire Kastler Brossel, École normale supérieure, 24, rue Lhomond, 75005 Paris, France*
[2] *Department of Physics, Bar Ilan University, 52900 Ramat Gan, Israel*
[3] *SKLQOQOD, Institute of Opto-Electronics, Shanxi University, Taiyuan 030006, P. R. China*

Summary. — We present an experimental study of the time of flight properties of a gas of ultra-cold fermions in the BEC-BCS crossover. Since interactions can be tuned by changing the value of the magnetic field, we are able to probe both non interacting and strongly interacting behaviors. These measurements allow us to characterize the momentum distribution of the system as well as its equation of state. We also demonstrate the breakdown of superfluid hydrodynamics in the weakly attractive region of the phase diagram, probably caused by pair breaking taking place during the expansion.

1. – Introduction

Feshbach resonances in ultra cold atomic gases offer the unique possibility of tuning interactions between particles, thus allowing one to study both strongly and weakly interacting many-body systems with the same experimental apparatus. A recent major achievement was the experimental exploration of the BEC-BCS crossover [1, 2, 3, 4, 5, 6], a scenario proposed initially by Eagles, Leggett, Nozières and Schmitt-Rink to bridge the gap between the Bardeen-Cooper-Schrieffer (BCS) mechanism for superconductivity in metals, and the Bose-Einstein condensation of strongly bound pairs [7, 8, 9]. Here, we present a study of the crossover using time of flight measurements. This technique gives access to a wide range of physical properties of the system and has been successfully used in different fields of physics. The observation of elliptic flows was for instance used to demonstrate the existence of quark-gluon plasmas in heavy ion collisions [10]. In cold atoms, the ellipticity inversion after free flight is a signature of Bose-Einstein condensation [11, 12]. In an optical lattice the occurrence of interference peaks can be used as the signature of the superfluid to insulator transition [13] and, with fermions, it can be used

© Società Italiana di Fisica

to image the Fermi surface [14]. Two series of time-of-flight measurements are presented: expansion of the gas without interactions, which gives access to the momentum distribution, a fundamental element in the BEC-BCS crossover, or with interactions, which allows us to characterize the equation of state of the system, and probe the validity of superfluid hydrodynamics.

2. – Experimental method

In a magnetic trap, a spin polarized gas of $N = 10^6$ ^{6}Li atoms in $|F = 3/2, m_F = +3/2\rangle$ is sympathetically cooled by collisions with ^{7}Li in $|F = 2, m_F = +2\rangle$ to a temperature of 10 μK. This corresponds to a degeneracy of $T/T_F \sim 1$, where $T_F = \hbar\bar{\omega}(6N)^{1/3}/k_{\mathrm{B}}$ is the Fermi temperature of the gas. The magnetic trap frequencies are 4.3 kHz (76 Hz) in the radial (axial) direction, and $\bar{\omega} = (\omega_x\omega_y\omega_z)^{1/3}$ is the mean frequency of the trap. Since there are no thermalizing collisions between the atoms in a polarized Fermi gas, the transfer into our final crossed dipole trap, which has a very different geometry (Fig. 1), is done in two steps. We first transfer the atoms into a mode-matched horizontal single beam Yb:YAG dipole trap, with a waist of ~ 23 μm. At maximum optical power (2.8 W), the trap depth is ~ 143 μK (15 T_F), and the trap oscillation frequencies are 6.2(1) kHz (63(1) Hz) in the radial (axial) direction. The atoms are transferred in their absolute ground state $|F = 1/2, m_F = +1/2\rangle$ by an RF pulse. We then sweep the magnetic field to 273 G and drive a Zeeman transition between $|F = 1/2, m_F = +1/2\rangle$ and $|F = 1/2, m_F = -1/2\rangle$ to prepare a balanced mixture of the two states (better than 5%). At this magnetic field, the scattering length between both states is $-280\,a_0$ (Fig. 2). After 100 ms the mixture has lost its coherence, initiating collisions in the gas. During the thermalization process about half of the atoms are lost. We then perform a final evaporative cooling stage by lowering the trap depth to $\sim 36\,\mu$K. At this point, we ramp up a vertical Nd:YAG laser beam (power 126 mW and waist $\sim 25\,\mu$m), obtaining our final crossed dipole trap configuration (Fig. 1). The measured degeneracy is $T/T_F \lesssim 0.15$. The magnetic field is then increased to 828 G (in the vicinity of the Feshbach resonance, see Fig. 2), where we let the gas thermalize for 200 ms before performing subsequent experiments.

3. – Momentum distribution

In standard BCS theory, the ground state of an homogeneous system is described by a pair condensate characterized by the many-body wave function

$$|\psi\rangle = \prod_{\boldsymbol{k}} (u_{\boldsymbol{k}} + v_{\boldsymbol{k}} a^{\dagger}_{\boldsymbol{k},\uparrow} a^{\dagger}_{-\boldsymbol{k},\downarrow})|0\rangle,$$

where $|0\rangle$ is the vacuum and $a^{\dagger}_{\boldsymbol{k},\sigma}$ is the creation operator of a fermion with momentum $\boldsymbol{k}$ and spin σ. In this expression, $|v_{\boldsymbol{k}}|^2$ can be interpreted as the occupation probability in momentum space, and is displayed in Fig. 3a for several values of the interaction

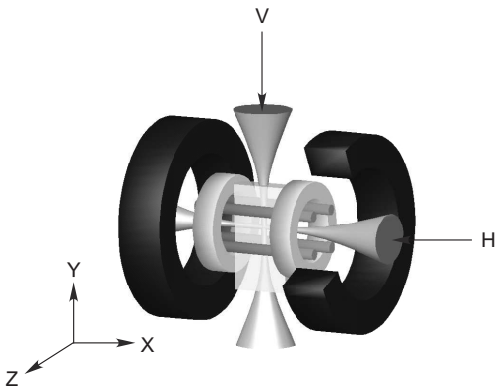

Fig. 1. – Ioffe-Pritchard trap and crossed dipole trap used for the experiments. The crossed geometry allows us to change the aspect ratio of the trap.

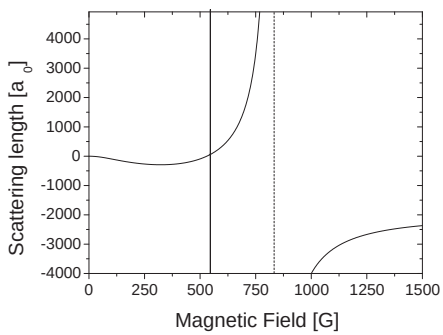

Fig. 2. – ^{6}Li Feshbach resonance between $|F = 1/2, m_F = +1/2\rangle$ and $|F = 1/2, m_F = -1/2\rangle$. The broad Feshbach resonance is located at 834 G. The balanced mixture is prepared at 273 G.

parameter $1/k_F a$, where k_F is the Fermi wave vector of the non interacting Fermi gas ($E_F = \hbar^2 k_F^2/2m$). One effect of the pairing of the atoms is to broaden the momentum distribution. In the BCS limit ($1/k_F a \to -\infty$), the broadening with respect to the momentum distribution of an ideal Fermi gas is very small, of the order of the inverse of the coherence length ξ. In the unitary limit ($1/k_F a \to 0$) it is expected to be of the order of k_F. In the BEC limit ($1/k_F a \to \infty$) we have molecules of size a so the momentum distribution, which is given by the Fourier transform of the molecular wave function, has a width $\hbar/a$.

In a first series of expansion experiments, we have measured the momentum distribution of a trapped Fermi gas in the BEC-BCS crossover. Similar experiments have been performed at JILA on ^{40}K [15].

In order to measure the momentum distribution of the atoms, the gas must expand freely, without any interatomic interactions. To achieve this, we quickly switch off the magnetic field so that the scattering length is brought to zero (see FIG. 2) [16]. We prepare $N = 3 \times 10^4$ atoms at 828 G in the crossed dipole trap with frequencies $\omega_x = 2\pi \times 2.78$ kHz, $\omega_y = 2\pi \times 1.23$ kHz and $\omega_z = 2\pi \times 3.04$ kHz. The magnetic field is adiabatically swept in 50 ms to different values in the crossover region. Then, we simultaneously switch off both dipole trap beams and the magnetic field (with a linear ramp of 296 G/μs). After 1 ms of free expansion, the atoms are detected by absorption imaging. The measured density profiles give directly the momentum distribution of the gas integrated along the imaging direction.

In FIG. 3, we show the measured momentum distributions for three different interaction parameters, corresponding to the BCS side of the resonance, the unitary limit and the BEC side of the resonance. Together with our data, we have plotted the predictions

of mean field BCS theory at $T = 0$, taking into account the trapping potential with a local density approximation [17]. k_F^0 is now the Fermi wave-vector calculated at the center of the harmonic trap for an ideal gas.

Some precautions need to be taken concerning this type of measurements due to possible density dependent losses during the magnetic field switch-off. If the magnetic field is not turned off fast enough, some atoms can be bound into molecules while the Feshbach resonance is crossed. The molecules are not detected with the imaging light and therefore will appear as a loss of the total number of atoms. Even if, as in our case, the Feshbach resonance is crossed in only 1 μs, this time may not be small compared to the typical many-body timescale ($\hbar/E_F \sim 1.3\,\mu s$ for Fig. 3 data).

To investigate quantitatively this effect, we have performed an additional experiment in a more tightly confining trap. We prepare a gas of 5.9×10^4 atoms at 828 G in a trap with frequencies $\omega_x = 2\pi \times 1.9$ kHz, $\omega_y = 2\pi \times 3.6$ kHz and $\omega_z = 2\pi \times 4.1$ kHz. The total peak density in the trap is 1.3×10^{14} atoms/cm^3. We let the gas expand at high field for a variable time t_B, then switch off B and detect the atoms after 0.5 ms of additional free expansion. Assuming hydrodynamic expansion at unitarity we calculate the density after t_B [18] and obtain the fraction of atoms detected as a function of the density of the gas when the resonance is crossed. For instance, we detect $\simeq 60\%$ fewer atoms for $t_B = 0$ compared to $t_B = 0.5$ ms, where the density is a factor $\simeq 10^3$ lower. The results are nicely fitted by a Landau-Zener model :

$$N_{\text{detected}}/N_{\text{total}} = \exp\left(-A\frac{n(t_B)}{2\dot{B}}\right),$$

where $n(t_B)$ is the total density at t_B, $\dot{B}$ the sweep rate and A the coupling constant between the atoms and the molecules. We determine $A \simeq 5 \times 10^{-12}$ G m^3/s. Our result is five times smaller than the MIT value $A \simeq 24 \times 10^{-12}$ G m^3/s [19], measured at a total peak density of 10^{13} atoms/cm^3 (one order of magnitude smaller than in our experiment). The theoretical prediction, assuming only two body collisions, is $A = 19 \times 10^{-12}$ G m^3/s [20]. The difference between our measurement and theory may suggest that many-body effects are important in our case. Finally, using our value of A the model predicts an atom number loss of about 27% for the momentum distribution measurements of Fig. 3. This loss is comparable to our shot-to-shot fluctuations in atom number and therefore was not unambiguously observed.

In conclusion, we have performed a measurement of the momentum distribution of a trapped Fermi gas. The results are found in reasonable agreement with BCS theory despite the fact that it is not expected to be quantitatively correct in the strongly interacting regime. In future work, experiments at lower density will be performed, in order to avoid the observed loss effect. This should allow us to distinguish between BCS and more exact theories [21]. It would also be interesting to perform measurements at different temperatures as in Ref. [22].

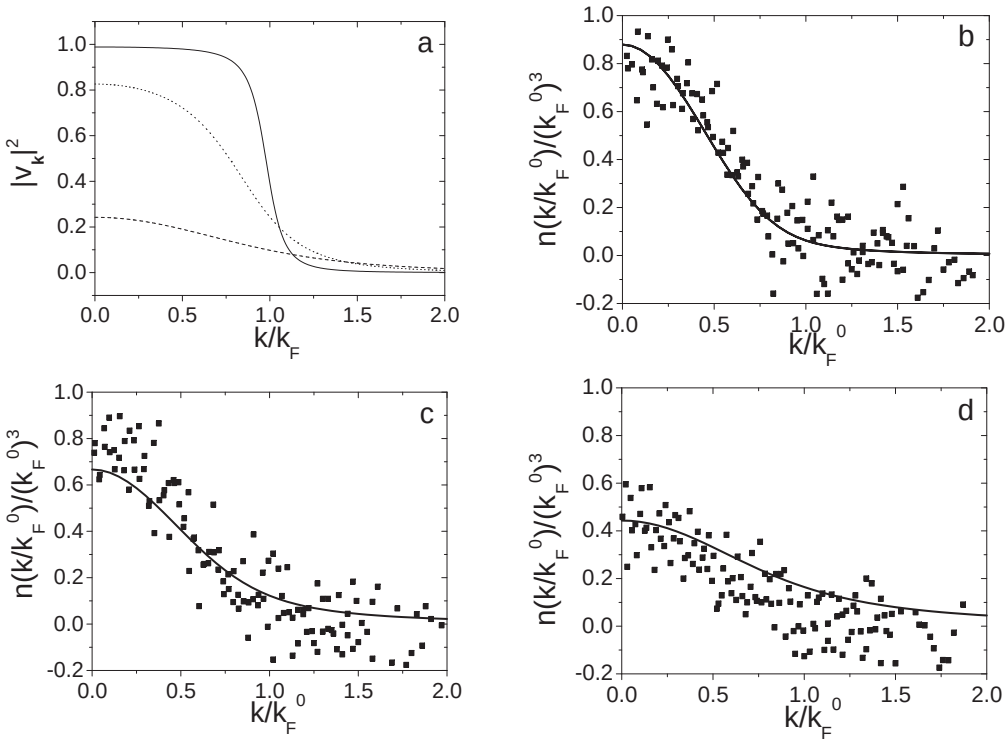

Fig. 3. – (a): Momentum distribution of a uniform Fermi gas for $1/k_F a = -1$ (solid line), $1/k_F a = 0$ (dotted line) and $1/k_F a = 1$ (dashed line) calculated from mean field BCS theory at $T = 0$ [17]. The results obtained from quantum Monte Carlo simulations [21] show that BCS theory slightly underestimates the broadening; (b): Measured momentum distribution of a trapped Fermi gas on the BCS side of the resonance ($1/k_F^0 a = -0.42$); (c): Unitary limit ($1/k_F^0 a = 0$); (d): BEC side of the resonance ($1/k_F^0 a = 0.38$). The solid lines in (b), (c) and (d) are the predictions of BCS mean field theory taking into account the trapping potential with a local density approximation [17]. k_F^0 is defined in the text.

4. – Release energy

In a second series of experiments, we have performed expansions at constant magnetic field, thus keeping the interactions present during the time of flight. The analysis of size measurement across the BEC-BCS crossover yields valuable information on the influence of interactions on the properties of the system. In particular, we have measured the release energy of the gas in the BEC-BCS crossover [3]. On resonance ($1/k_F^0 a = 0$), the gas reaches a universal behavior [23]. The chemical potential μ is proportional to the Fermi energy $\mu = (1 + \beta)E_F$. We have determined the universal scaling parameter β from our release energy measurement.

The starting point for the experiment is a nearly pure molecular condensate of 7×10^4 atoms at 770 G, in an optical trap with frequencies $\omega_x = 2\pi \times 830$ Hz, $\omega_y = 2\pi \times 2.4$ kHz, and $\omega_z = 2\pi \times 2.5$ kHz. We slowly sweep the magnetic field at a rate of 2 G/ms to various values across the Feshbach resonance. We detect the integrated density profile after a time of flight expansion of 1.4 ms in several stages: 1 ms of expansion at high magnetic field, followed by a fast ramp of 100 G in 50 μs in order to dissociate the molecules and, after the fast switch-off of the magnetic field, 350 μs of ballistic expansion.

Fig. 4 presents the gas energy released after expansion, which is calculated from gaussian fits to the optical density after time of flight: $E'_{\rm rel} = m(2\sigma_y^2 + \sigma_x^2)/2\tau^2$, where σ_i is the rms width along i and τ is the time of flight. We assume that the size σ_z (which is not observed) is equal to σ_y. Note that both in the weakly interacting case and unitarity limit the density has a Thomas-Fermi profile and the release energy can be calculated from the exact profiles. However, we have chosen this gaussian shape to describe the whole crossover region with a single fit function. This leads to a rescaling of the release energy. In particular, the ideal Fermi gas release energy in an harmonic trap is $E_{\rm rel} = 3/8 E_F$ but when using the gaussian fit to the Thomas-Fermi profile we get instead $E'_{\rm rel} = 0.46 E_F$ as shown in Fig. 4.

The release energy in the BEC-BCS crossover varies smoothly. It presents a plateau for $-1/k_F a \leq -0.5$, (BEC side) and then increases monotonically towards that of a weakly interacting Fermi gas. On resonance, the release energy scales as $E_{\rm rel} = \sqrt{1+\beta}\, E^0_{\rm rel}$, where $E^0_{\rm rel}$ is the release energy of the non interacting Fermi gas. The square root comes from the average over the trap. At 834 G, we get $\beta = -0.59(15)$. This value is slightly different from our previous determination $\beta = -0.64(15)$, where the resonance was assumed to be located at 820 G instead of 834 G [3]. Our result agrees with other measurements performed on ^{6}Li and with some theoretical predictions (see Table I). Remarkably, the recent ^{40}K measurement at JILA is also in very good agreement, thus proving the universality of the unitarity regime.

5. – Ellipticity

Nontrivial information can be extracted from the measurement of the aspect ratio of the cloud after expansion. For instance, in the first days of gaseous Bose-Einstein condensates, the onset of condensation was characterized by an ellipticity inversion after time of flight, a dramatic effect compared to the isotropic expansion of a non condensed Boltzmann gas. In the case of strongly interacting Fermi gases, ellipticity measurements can be used as probes for the hydrodynamic behavior of the system, and constitute an indirect signature of the appearance (or breakdown) of superfluidity.

We have studied the ellipticity of the cloud as a function of the magnetic field for different temperatures. As before, the density profiles are fitted with gaussians, and the ellipticity is defined as $\eta = \sigma_y/\sigma_x$. We prepare $N = 3 \times 10^4$ atoms at 828 G in a crossed dipole trap. The magnetic field is adiabatically swept in 50 ms to different values in the crossover region. Then, we switch off both dipole trap beams and let the gas expand

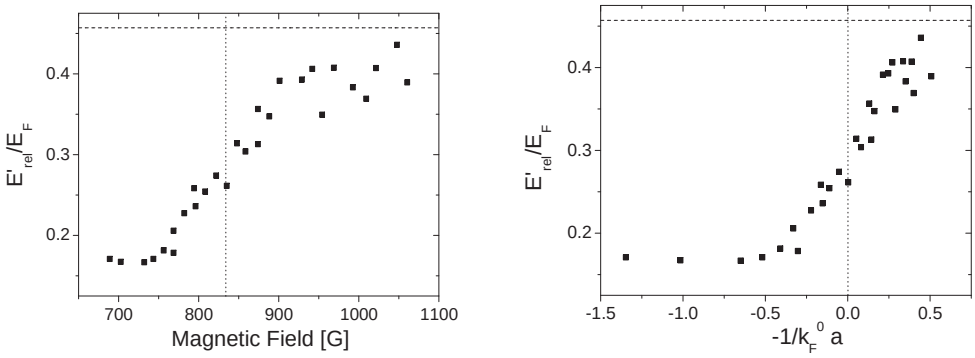

Fig. 4. – Rescaled release energy $E'_{\rm rel}$ of a trapped Fermi gas in the BEC-BCS crossover as a function of the magnetic field and as a function of $-1/k_F^0 a$ [3]. The dashed line is the rescaled release energy of a $T = 0$ non interacting Fermi gas. From the measurement at resonance we extract $\beta = -0.59(15)$.

		β
Experimental results on ^{6}Li at finite T	This work	$-0.59(15)$
	ENS 2004 [3]	$-0.64(15)$
	Innsbruck [24]	$-0.73^{+12}_{-0.09}$
	Duke [25]	$-0.49(4)$
	Rice [26]	$-0.54(5)$
Experimental result on ^{40}K extrapolation to T=0	JILA [27]	$-0.54^{+0.05}_{-0.12}$
Theoretical predictions at $T = 0$	BCS theory [7, 8, 9]	-0.41
	Astrakharchik *et al.* [28]	$-0.58(1)$
	Carlson *et al.* [29, 30]	$-0.58(1)$
	Perali *et al.* [31]	-0.545
	Padé approximation [23, 32]	-0.67
	Steel [33]	-0.56
	Haussmann *et al.* [34]	-0.64
Theoretical predictions at $T = T_c$	Bulgac *et al.* [35]	-0.55
	Burovski *et al.* [36]	$-0.507(14)$

TABLE I. – *List of the recent experimental measurements and theoretical predictions of the universal scaling parameter β.*

for 0.5 ms in the presence of the magnetic field. After 0.5 ms of additional expansion at $B = 0$, the atoms are detected by absorption imaging. Fig. 5a and Fig. 5b show the measured value of the ellipticity as a function of the magnetic field for two different samples, which are at different temperatures. Together with the experimental results we have plotted the expected anisotropy from superfluid hydrodynamics [18]. For this, we have extracted from the quantum Monte Carlo simulation of ref. [28] the value of the polytropic exponent γ, defined as $\gamma = \frac{n}{\mu}\frac{\partial \mu}{\partial n}$.

The first series of measurements is done in a trap with frequencies $\omega_x = 2\pi \times 1.39$ kHz, $\omega_y = 2\pi \times 3.09$ kHz, $\omega_z = 2\pi \times 3.38$ kHz and trap depth $\sim 1.8\, T_F$. The measured ellipticity (Fig. 5a) is in good agreement with the hydrodynamic prediction on the BEC side, at resonance and on the BCS side until $1/k_F^0 a = -0.15$. It then decreases monotonically to 1.1 at $1/k_F^0 a = -0.5$.

For the second series of experiments we prepare a colder sample in a trap with frequencies $\omega_x = 2\pi \times 1.24$ kHz, $\omega_y = 2\pi \times 2.76$ kHz, $\omega_z = 2\pi \times 3.03$ kHz and trap depth $\sim 1.6\, T_F$. In this case the behavior of the anisotropy is very different (Fig. 5b). We observe a plateau until $1/k_F^0 a = -0.33$, in good agreement with the hydrodynamic prediction, and at this critical magnetic field there is a sharp decrease of η to a value close to 1.2. This sharp transition seems analogous to the sudden increase of the damping of the breathing mode observed in Innsbruck [37].

In a third experiment, we measure the ellipticity at unitarity as a function of trap depth (hence of the gas temperature). Below a critical trapping laser intensity, the ellipticity jumps from a low value (1.1) to the hydrodynamic prediction 1.45.

In all cases, the decrease of the anisotropy indicates a breakdown of superfluid hydrodynamics in the weakly attractive part of the phase diagram or at higher temperature. A first possibility would be that the gas crosses the critical temperature in the trap. However, we know from the MIT experiment [38] that pair breaking can occur during the expansion. During the time of flight, both the density and k_F decrease. On the BEC side of resonance, the binding energy of the molecules ($-\hbar^2/ma^2$) does not depend on the density and the pairs are very robust. By contrast, on the BCS side of resonance the generalized Cooper pairs become fragile as the gap decreases with $1/k_F a$ and they can be broken during the expansion. Our experiments use the ellipticity of the cloud as a probe and are complementary to the MIT approach, where the breakdown of superfluidity was characterized by the disappearance of vortices during the expansion of the gas. We are planning additional experiments in order to investigate wether the breakdown of superfluidity occurs in the trap or during the expansion.

6. – Conclusion

The results presented here constitute a first step in the understanding of the free flight properties of strongly correlated fermionic systems. In future work, we will investigate more thoroughly the pair breaking mechanism taking place during the expansion in the BCS part of the phase diagram. We point out the need for a dynamic model of the

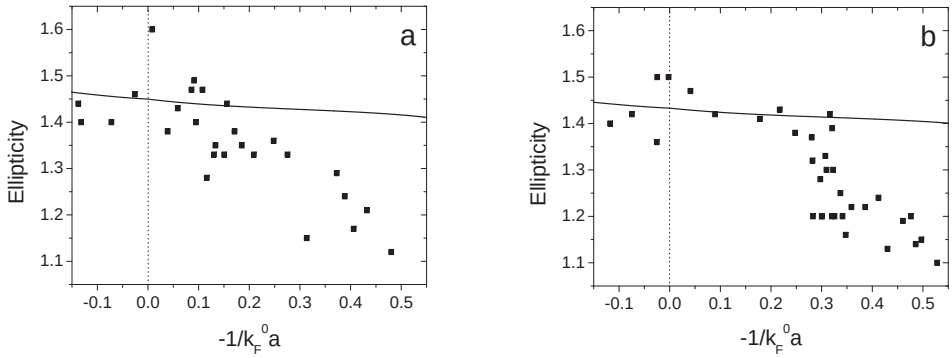

Fig. 5. – Ellipticity of the gas after expansion from a trap of depth $\sim 1.8\,T_F$(a) and from a trap of depth $\sim 1.6\,T_F$ (b). Solid lines: hydrodynamic predictions.

expanding gas at finite temperature.

7. – Acknowledgments

We gratefully acknowledge support by the IFRAF institute and the ACI Nanosciences 2004 NR 2019. We thank the ENS ultracold atoms group, S. Stringari, R. Combescot, D. Petrov and G. Shlyapnikov for stimulating discussions. Laboratoire Kastler Brossel is a research unit No. 8552 of CNRS, ENS, and Université Paris 6.

REFERENCES

[1] S. Jochim, M. Bartenstein, A. Altmeyer, G. Hendl, S. Riedl, C. Chin, J. Hecker Denschlag, and R. Grimm, *Science*, **302** (2003) 2101.
[2] M. Greiner, C. A. Regal, and D. S. Jin, *Nature*, **426** (2003) 537.
[3] T. Bourdel, L. Khaykovich, J. Cubizolles, J. Zhang, F. Chevy, M. Teichmann, L. Tarruell, S. J. J. M. F. Kokkelmans, and C. Salomon, *Phys. Rev. Lett.*, **93** (2004) 050401.
[4] M. W. Zwierlein, C. A. Stan, C. H. Schunck, S. M. F. Raupach, S. Gupta, Z. Hadzibabic, and W. Ketterle, *Phys. Rev. Lett.*, **91** (2003) 250401.
[5] J. Kinast, S. L. Hemmer, M. E. Gehm, A. Turlapov, and J. E. Thomas, *Phys. Rev. Lett.*, **92** (2004) 150402.
[6] G. B. Partridge, K. E. Strecker, R. I. Kamar, M. W. Jack, and R. G. Hulet, *Phys. Rev. Lett.*, **95** (2005) 020404.
[7] D. M. Eagles, *Phys. Rev.*, **186** (1969) 456.
[8] A. J. Leggett, in Modern Trends in the Theory of Condensed Matter, Lecture Notes in Physics Vol. 115, edited by A. Pekalski and R. Przystawa, (Springer-Verlag, Berlin) 1980, p. 13.
[9] P. Nozières and S. Schmitt-Rink, *J. Low Temp. Phys.*, **59** (1985) 195.

[10] E. Shuryak, *Prog. Part. Nucl. Phys.*, **53** (2004) 273.
[11] M. H. Anderson, J. R. Ensher, M. R. Matthews, C. E. Wieman and E. A. Cornell, *Science*, **269** (1995) 198.
[12] K. B. Davis, M.-O. Mewes, M. R. Andrews, N. J. van Druten, D. S. Durfee, D. M. Kurn and W. Ketterle, *Phys. Rev. Lett.*, **75** (1995) 3969.
[13] M. Greiner, O. Mandel, T. Esslinger, T. W. Hänsch, and I. Bloch, *Nature*, **415** (2002) 39.
[14] M. Köhl, H. Moritz, T. Stöferle, K. Günter, and T. Esslinger, *Phys. Rev. Lett.*, **94** (2005) 080403.
[15] C. A. Regal, M. Greiner, S. Giorgini, M. Holland, and D. S. Jin, *Phys. Rev. Lett.*, **95** (2005) 250404.
[16] T. Bourdel, J. Cubizolles, L. Khaykovich, K. M. F. Magalhães, S. J. J. M. F. Kokkelmans, G. V. Shlyapnikov, and C. Salomon, *Phys. Rev. Lett.*, **91** (2003) 020402.
[17] L. Viverit, S. Giorgini, L. Pitaevskii, and S. Stringari, *Phys. Rev. A*, **69** (2004) 013607.
[18] C. Menotti, P. Pedri, and S. Stringari, *Phys. Rev. Lett.*, **89** (2002) 250402.
[19] M. Zwierlein, PhD. Thesis, MIT (2006), p.107.
[20] J. Chwedeńczuk, K. Góral, T. Köhler, and P. Julienne, *Phys. Rev. Lett.*, **93** (2004) 260403.
[21] G. E. Astrakharchik, J. Boronat, J. Casulleras, and S. Giorgini, *Phys. Rev Lett.*, **95** (2005) 230405
[22] Q. Chen, C. A. Regal, D. S. Jin and K. Levin, *Phys. Rev. A*, **74** (2006) 011601.
[23] H. Heiselberg, *Phys. Rev. A*, **63** (2001) 043606
[24] M. Bartenstein, A. Altmeyer, S. Riedl, S. Jochim, C. Chin, J. H. Denschlag, and R. Grimm, *Phys. Rev. Lett.*, **92** (2004) 120401; revised value M. Bartenstein, PhD. Thesis, Universität Innsbruck, (2005), p.100.
[25] J. Kinast, A. Turlapov, J. Thomas, Q. Chen, J. Stajic, and K. Levin, *Science*, **307** (2005) 1296.
[26] G. B. Partridge, W. Li, R. I. Kamar, Y. Liao, and R. G. Hulet, *Science*, **311** (2005) 503.
[27] J. T. Stewart, J. T. Gaebler, C. A. Regal, and D. S. Jin, *Phys. Rev. Lett.*, **97** (2006) 220406.
[28] G. E. Astrakharchik, J. Boronat, J. Casulleras, and S. Giorgini, *Phys. Rev. Lett.*, **93** (2004) 200404.
[29] J. Carlson, S.-Y. Chang, V. R. Pandharipande, and K. E. Schmidt, *Phys. Rev. Lett.*, **91** (2003) 050401.
[30] J. Carlson and S. Reddy, *Phys. Rev. Lett.*, **95** (2005) 060401.
[31] A. Perali, P. Pieri, and G. C. Strinati, *Phys. Rev. Lett.*, **93** (2004) 100404.
[32] G. A. Baker, Jr., *Phys. Rev. C*, **60** (1999) 054311.
[33] J. V. Steele, e-print nucl-th/0010066.
[34] R. Haussmann, W. Rantner, S. Cerrito, and W. Zwerger, e-print cond-mat/0608282.
[35] A. Bulgac, J. E. Drut, and P. Magierski, *Phys. Rev. Lett.*, **96** (2006) 090404.
[36] E. Burovski, N. Prokof'ev, B. Svistunov, and M. Troyer, *Phys. Rev. Lett.*, **96** (2006) 160402.
[37] M. Bartenstein, A. Altmeyer, S. Riedl, S. Jochim, C. Chin, J. Hecker Denschlag, and R. Grimm, *Phys. Rev. Lett.*, **92** (2004) 203201.
[38] C. H. Schunck, M. W. Zwierlein, A. Schirotzek, and W. Ketterle, e-print cond-mat/0607298.